Large enhancement of second-harmonic generation in subwavelength metal-dielectric-metal plasmonic waveguides

Georgios Veronis[1] and Shanhui Fan[2]

[1]Department of Electrical and Computer Engineering and Center for Computation and Technology, Louisiana State University, Baton Rouge, LA 70803

[2]Department of Electrical Engineering, Stanford University, Stanford, California 94305

ABSTRACT

Plasmonic waveguides have shown the potential to guide subwavelength optical modes, the so called surface plasmon polaritons, at metal-dielectric interfaces. In particular, a metal-dielectric-metal (MDM) structure supports a subwavelength propagating mode at a wavelength range extending from DC to visible. Thus, such a waveguide could be important in providing an interface between conventional optics and subwavelength electronic and optoelectronic devices. Nonlinear processes such as second-harmonic generation (SHG) are important for applications such as switching and wavelength conversion. In this paper, we show that field enhancement in MDM waveguides can result in large enhancement of SHG. We first consider a structure consisting of a MDM waveguide filled with lithium niobate, which is sandwiched between two high-index-contrast dielectric waveguides. Such a structure forms a Fabry-Perot resonant cavity and can be designed to have a resonance at both the first and second harmonic. We show that this doubly resonant device results in more than two orders of magnitude enhancement in SHG compared to a uniform slab of lithium niobate. We also consider structures in which multisection tapers are used to couple light in and out of the MDM waveguide. We optimize the tapers so that their transmission efficiency is maximized at both the first and second harmonic. For such structures the field enhancement is due to the squeezing of the optical power from the wavelength-sized dielectric waveguide to the deep subwavelength MDM waveguide.

Keywords: Plasmonic devices, subwavelength optical devices, couplers

1. INTRODUCTION

Plasmonic waveguides have shown the potential to guide subwavelength optical modes, the so-called surface plasmon polaritons, at metal-dielectric interfaces. Several different plasmonic waveguiding structures have been proposed,[1–6] such as metallic nanowires[2,3] and metallic nanoparticle arrays.[4,5] Most of these structures support a highly-confined mode only near the surface plasmon frequency. In this regime, the optical mode typically has low group velocity and short propagation length. It has been shown however that a metal-dielectric-metal (MDM) structure with a dielectric region thickness of $\sim$100 nm supports a propagating mode with a nanoscale modal size at a wavelength range extending from DC to visible.[7] Thus, such a waveguide could be potentially important in providing an interface between conventional optics and subwavelength electronic and optoelectronic devices.

Because of the predicted attractive properties of MDM waveguides, people have started to explore such structures experimentally. In particular, Dionne *et al.*[8] have recently demonstrated waveguiding in a quasi-two-dimensional MDM geometry experimentally, showing clear evidence of a subwavelength guided mode with substantial propagation distances. With this as a background, it is important to explore the coupling of a dielectric slab waveguide into such a quasi-two-dimensional MDM geometry.

In this paper, we show that field enhancement in MDM waveguides can result in large enhancement of SHG. We first consider a structure consisting of a MDM waveguide filled with lithium niobate, which is sandwiched between two high-index-contrast dielectric waveguides. Such a structure forms a Fabry-Perot resonant cavity and can be designed to have a resonance at both the first and second harmonic. We show that this doubly resonant device results in more than two orders of magnitude enhancement in SHG compared to a uniform slab of lithium niobate. We also consider structures in which multisection tapers are used to couple light in and out of the MDM waveguide. We optimize the tapers so that their transmission efficiency is maximized at both the

Integrated Optics: Devices, Materials, and Technologies XIII, edited by Jean-Emmanuel Broquin, Christoph M. Greiner,
Proc. of SPIE Vol. 7218, 72180Y · © 2009 SPIE · CCC code: 0277-786X/09/$18 · doi: 10.1117/12.809727

first and second harmonic. For such structures the field enhancement is due to the squeezing of the optical power from the wavelength-sized dielectric waveguide to the deep subwavelength MDM waveguide.

The remainder of the paper is organized as follows. In Section 2 we describe the simulation methods used for the analysis of the coupler structures. The results obtained using these methods for the various coupler designs are presented in Section 3.

2. SIMULATION METHOD

We use a two-dimensional finite-difference frequency-domain (FDFD) method[9, 10] to theoretically investigate the properties of the couplers. This method allows us to directly use experimental data for the frequency-dependent dielectric constant of metals such as silver,[11] including both the real and imaginary parts, with no further approximation. Perfectly matched layer (PML) absorbing boundary conditions are used at all boundaries of the simulation domain.[12] Due to the rapid field variation at the metal-dielectric interfaces, a very fine grid resolution of $\sim$1 nm is required at the metal-dielectric interfaces to adequately resolve the local fields. On the other hand, a grid resolution of $\sim \lambda/20$ is sufficient in the dielectric waveguide regions of the simulation domain. For example the required grid size in air at λ_0 =1.55 μm is $\sim$77.5 nm which is almost two orders of magnitude larger than the required grid size at metal-dielectric interfaces. We therefore use a nonuniform orthogonal grid[13] to avoid an unnecessary computational cost. We found that by using such a grid our results are accurate to $\sim$0.05%.

In all cases the dielectric and plasmonic waveguides are aligned with their axes coinciding. To calculate the transmission and reflection coefficients of couplers between dielectric and MDM plasmonic waveguides, we excite the fundamental mode at the input waveguide and measure the power flux at both the input and output waveguides. These fluxes are then normalized with respect to the incident power flux in the input waveguide. We excite the fundamental TM mode of the dielectric waveguide by a line source with the appropriate mode profile calculated by solving the modal dispersion relation. We define the *transmission efficiency* of the coupler T_{ij} as the ratio of the transmitted power into the fundamental mode of the output waveguide j, and of the incident power of the fundamental mode of the input waveguide i.

We use FDFD and the undepleted-pump approximation to calculate the SHG power guided in the output silica-silicon-silica dielectric waveguide. We also calculate the SHG power for the same volume of nonlinear material in a uniform thick slab and for a power density equal to the average power density in the silicon core of the input dielectric waveguide. The ratio between these two SHG powers defines the enhancement factor of SHG.

3. RESULTS

3.1. Fabry-Perot structure for enhanced second harmonic generation

We first consider a Fabry-Perot cavity structure consisting of a MDM waveguide filled with lithium niobate, which is sandwiched between two silica-silicon-silica dielectric waveguides [Fig. 1(a)]. Such a device could be used for nonlinear optics applications on chip. In such devices the squeezing of the optical power from the wavelength-sized dielectric waveguide into the deep subwavelength MDM waveguide leads to field enhancement. In addition, the MDM waveguide sandwiched between the two dielectric waveguides forms a Fabry-Perot resonant cavity. Thus, in addition to the field enhancement due to the increased field concentration in the MDM waveguide, the field can be further enhanced when the resonance condition of the Fabry-Perot cavity is satisfied. The field enhancement leads to enhanced SHG.

In Fig. 2(b) we show the SHG enhancement factor for the structure of Fig. 2(a) as a function of wavelength. We observe that there is significant enhancement of SHG over a broad wavelength range with a maximum enhancement factor of 100. The reflections at the interfaces between the MDM waveguide and the dielectric slab waveguides lead to Fabry-Perot oscillations in the transmission efficiency of both the first and the second harmonic. These result in the strong dependence of the SHG enhancement factor on wavelength [Fig. 2(b)].

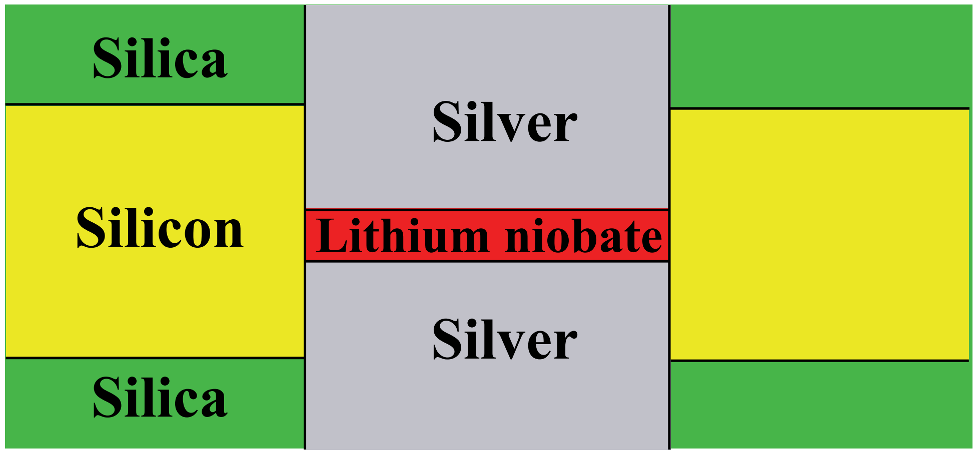

(a)

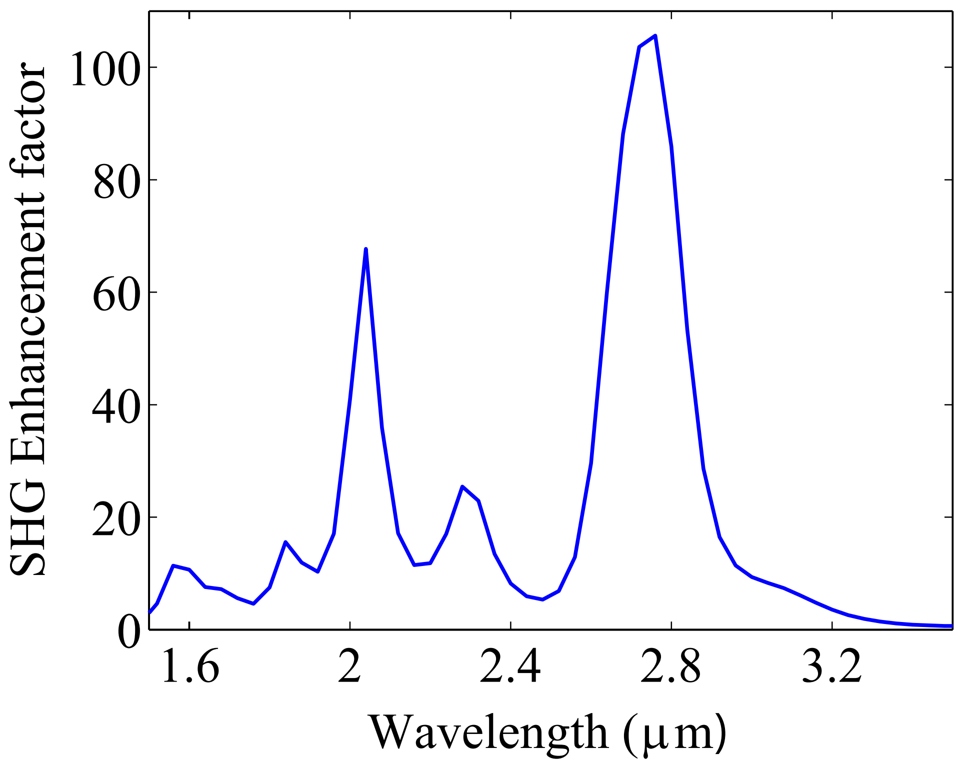

(b)

Figure 1. (a) Schematic of a Fabry-Perot cavity structure consisting of a MDM waveguide sandwiched between two silica-silicon-silica dielectric waveguides. The MDM waveguide is filled with lithium niobate which has a large nonlinear susceptibility. (b) Enhancement factor of second harmonic generation as a function of wavelength calculated using FDFD. Results are shown for wd=300 nm, wp=25 nm, lp=1 m.

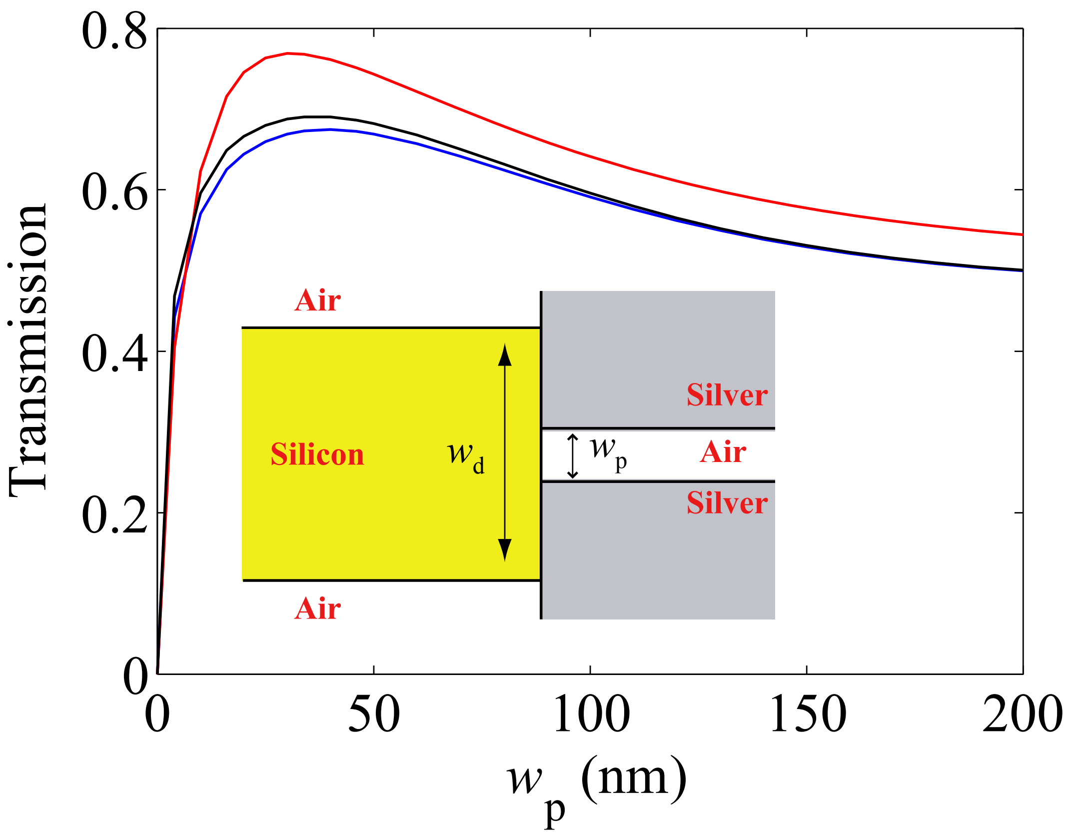

Figure 2. Power transmission efficiency (blue line) of a coupler between a dielectric and a MDM waveguide as a function of the width of the plasmonic waveguide w_p at λ_0 =1.55 μm calculated using FDFD. The coupler, created by placing the dielectric waveguide terminated flat at the exit end of the MDM waveguide, is shown in the inset. Results are shown for w_d = 300 nm. Also shown is the transmission efficiency, if the metal in the MDM waveguide is lossless (black line), or perfect electric conductor (red line).

3.2. Direct coupling

The large SHG in the Fabry-Perot structure is associated with the high coupling efficiency between the dielectric and the plasmonic MDM waveguide. We consider a coupler created by simply placing an air-silicon-air dielectric slab waveguide terminated flat at the exit end of a two-dimensional silver-air-silver MDM plasmonic waveguide (inset of Fig. 2). In Fig. 2 we show the coupler transmission $T_{dp}(= T_{pd})$ as a function of the width of the plasmonic waveguide w_p at λ_0 =1.55 μm. The width of the dielectric waveguide is w_d = 300 nm, which approximately corresponds to the optimal width of a silicon slab waveguide surrounded by air that achieves the minimum TM modal size. We observe that the transmission efficiency in this coupler is high and the maximum transmission of 68% is obtained for $w_p \simeq$40 nm. The transmission is also weakly dependent on w_p for $w_p >$20 nm. At the limit $w_p \rightarrow$0 the transmission goes to zero as expected. In Fig. 2 we also show the transmission for a coupler in which the metal in the MDM waveguide is lossless ($\epsilon_{\text{met}} = \epsilon_{\text{met,real}}$, neglecting the imaginary part of the dielectric permittivity $\epsilon_{\text{met,imag}}$) or perfect electric conductor (PEC) ($\epsilon_{\text{met}} = -\infty$). In the former case we observe that the material losses in the metal do not affect significantly the transmission efficiency of the coupler. In the latter case (PEC), the transmission of the coupler is slightly higher, and its dependence on the MDM waveguide width is very similar to the plasmonic case. At λ_0 =1.55 μm the penetration of the electric field into the metal region is weak, and thus a PEC model provides a reasonable qualitative approximation.

In general we found that for a given width of the subwavelength MDM waveguide w_p, there is an optimum width of the dielectric waveguide w_d which maximizes the transmission efficiency and vice versa. We also found that for a given w_d the optimum w_p is significantly smaller than w_d. This is due to the fact that a subwavelength MDM waveguide collects light from an area significantly larger than its cross-sectional area.[14] More precisely, the transmission cross section of a MDM waveguide (in the unit of length in two dimensions), defined as the transmitted power into the waveguide normalized by the incident plane wave power flux, is significantly larger than its geometric cross-sectional area. As an example, we found that the transmission cross section of a MDM waveguide with w_p =50 nm is $\sim$185 nm at λ_0 =1.55 μm. On the other hand, the transmission cross section of dielectric waveguides is approximately equal to their geometrical area. For example, for a waveguide consisting of a silicon slab surrounded by air with w_d =320 nm we found that the transmission cross section is $\sim$340 nm at λ_0 =1.55 μm.

We also note that almost perfect transmittance has been previously reported for metallic grating structures, consisting of a periodic arrangement of subwavelength slits on a metal film.[15–17] It has also been shown that enhanced transmission is also present in single subwavelength slits,[18] and that the transmission can be further enhanced by corrugating the metal surface in the vicinity of the slit.[19] In all these previous studies the transmission was calculated for a plane wave excitation. In contrast, in our case the light funneling is provided by the dielectric waveguide.

In Figs. 3a and 3b we show the profiles of the magnetic and electric field respectively for a coupler with w_d =300 nm, w_p =50 nm (Fig. 1a). The power is incident from the left so that the incident and reflected waves result in an interference pattern in the dielectric waveguide. We note that the electric field intensity is significantly enhanced in the MDM waveguide with respect to the dielectric waveguide, while similar enhancement is not observed for the magnetic field intensity. This can be understood if we note that from Maxwell's equations we have $E_y = -\frac{1}{j\omega\epsilon}\frac{\partial H_z}{\partial x} = \frac{\gamma}{j\omega\epsilon}H_z$, so that for the Poynting vector we have $S = \frac{1}{2}\text{Re}(E_y H_z^*) \propto \frac{\beta}{\omega\epsilon}|H_z|^2 \propto \frac{\omega\epsilon}{\beta}|E_y|^2$, where $\gamma = \alpha + j\beta$ is the propagation constant of the mode. Thus, for the magnetic field enhancement we have $|\frac{H_{zp}}{H_{zd}}|^2 \sim \frac{w_d}{w_p}\frac{\beta_d/\epsilon_d}{\beta_p/\epsilon_p}$, while for the electric field enhancement we have $|\frac{E_{yp}}{E_{yd}}|^2 \sim \frac{w_d}{w_p}\frac{\epsilon_d/\beta_d}{\epsilon_p/\beta_p}$. The observed field enhancements (Fig. 3) are consistent with these relations.

3.3. Multisection taper

As mentioned above, a simple coupler created by placing a dielectric waveguide terminated flat at the exit end of a MDM waveguide (inset of Fig. 2), can be designed to have transmission efficiency of 68%. To further increase the transmission, we design a coupler consisting of a multisection taper shown in Fig. 4a. Such tapers, consisting of a number of waveguide sections, have been used as couplers between dielectric waveguides with highly different widths.[20–22] It has been shown theoretically and confirmed experimentally that they can be designed to have higher transmission efficiency than conventional tapers of the same length with linear or parabolic shapes.[21,22] The coupler design used here consists of a number of dielectric waveguide and MDM waveguide sections. The

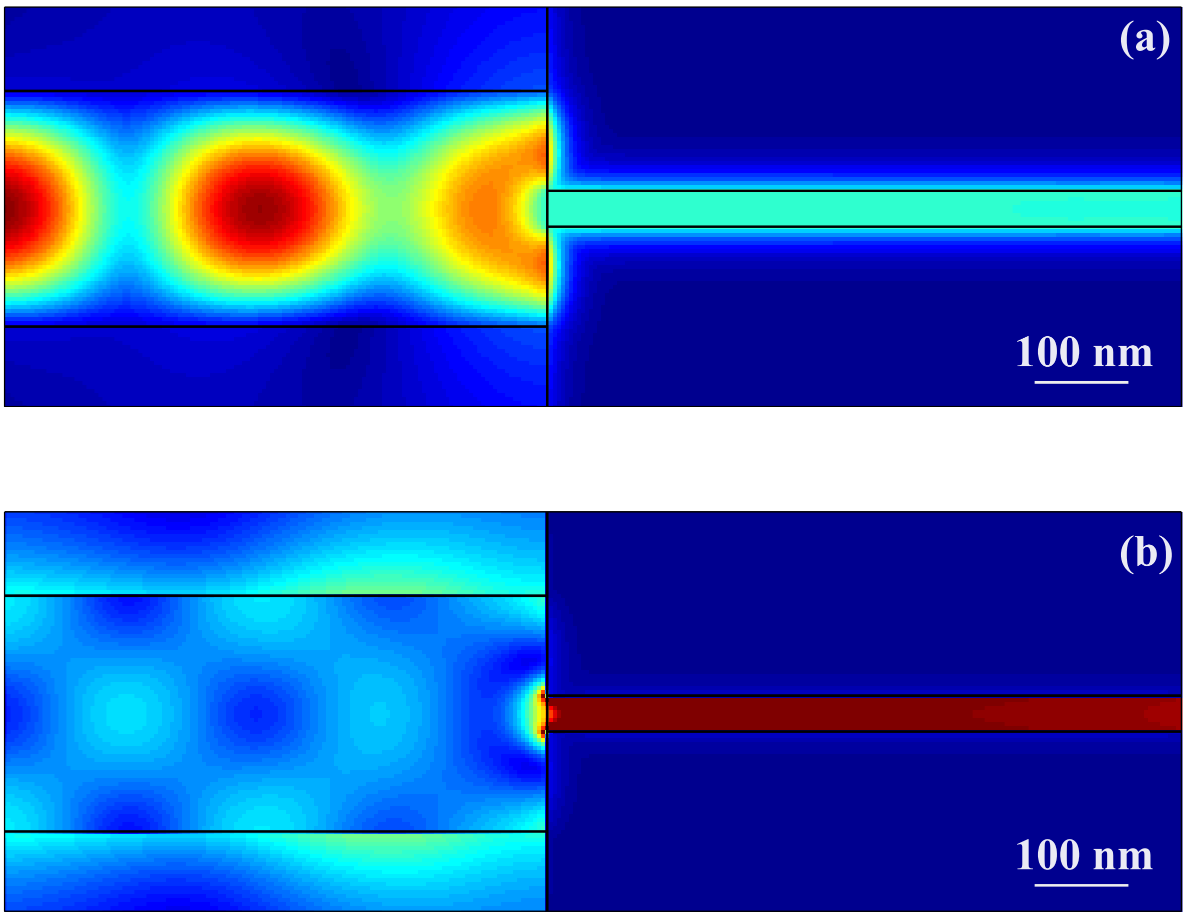

Figure 3. (a) Profile of the magnetic field amplitude $|H|$ for w_d =300 nm, w_p =50 nm (Fig. 1a). (b) Profile of the electric field amplitude $|E|$ for w_d =300 nm, w_p =50 nm.

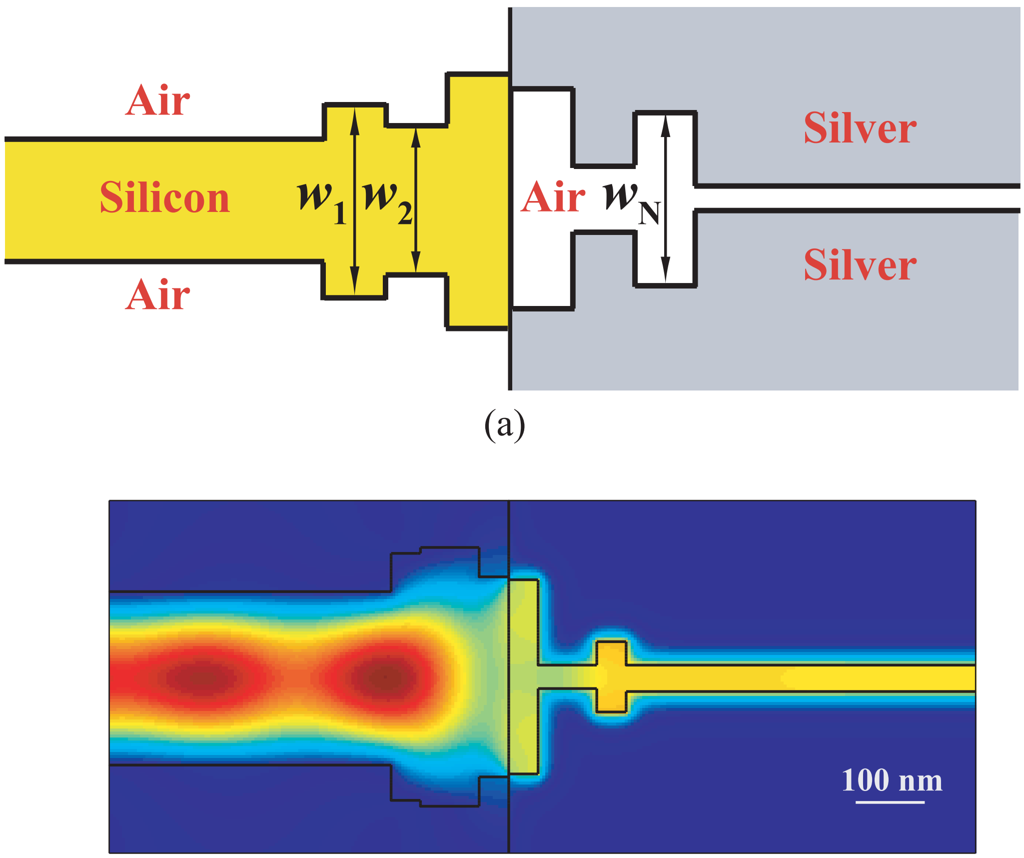

(a)

(b)

Figure 4. (a) Schematic of a coupler consisting of a multisection taper. (b) Profile of the magnetic field amplitude $|H|$ of the optimized coupler design for w_d =300 nm, w_p =50 nm and 8 waveguide sections. The optimized widths of the dielectric waveguide sections are w_1 =420 nm, w_2 =440 nm, w_3 =440 nm, w_4 =340 nm, while the widths of the MDM waveguide sections are w_5 =330 nm, w_6 =40 nm, w_7 =40 nm, w_8 =120 nm.

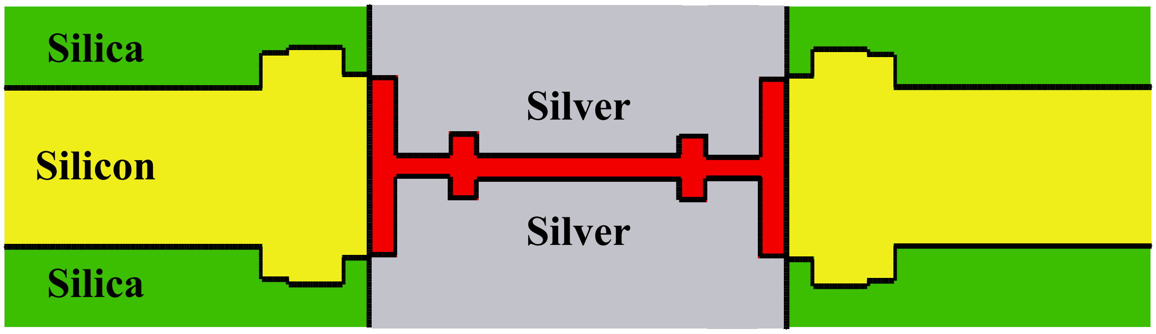

(a)

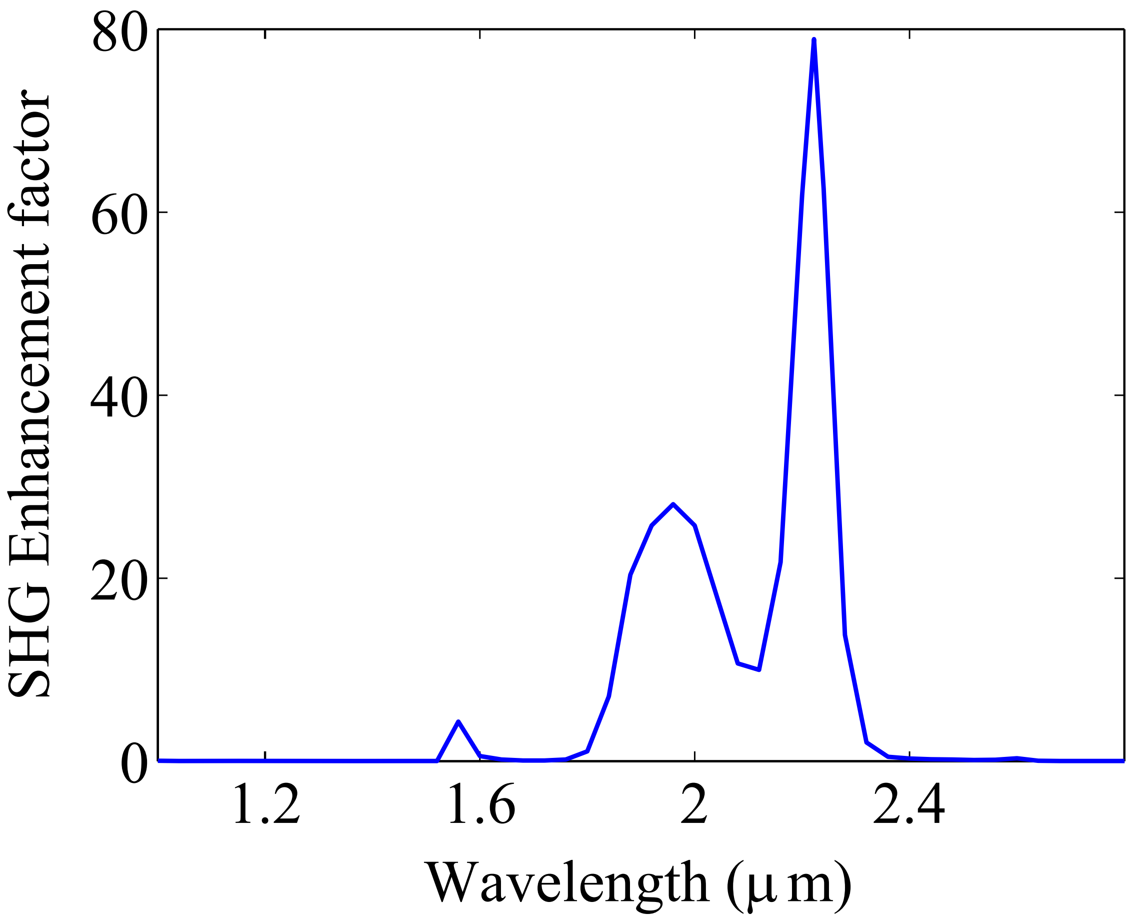

(b)

Figure 5. (a) Schematic of nonlinear devices in which multisection tapers are used as couplers between the MDM and dielectric waveguides. (b) Enhancement factor of second harmonic generation as a function of wavelength calculated using FDFD. Results are shown for wd=300 nm, wp=25 nm.

widths of these sections are optimized using a genetic global optimization algorithm in combination with FDFD. More specifically, we use a microgenetic algorithm which has been shown to reach the near-optimal region much faster than large population genetic algorithms.[23,24] Using this approach we designed a coupler with 93% transmission efficiency for w_d =300 nm, w_p =50 nm at λ_0 =1.55 μm. In this design we use 4 dielectric waveguide sections and 4 MDM waveguide sections. The lengths of all waveguide sections are l_i =50 nm. Their widths $w_1, w_2, ..., w_8$ are optimized using the microgenetic algorithm, while the number of dielectric and MDM sections as well as their lengths are kept fixed during the optimization process. The designed coupler is extremely compact with a total length of 400 nm. The magnetic field profile for this optimized coupler design is shown in Fig. 4b.

Both the simple coupler of Fig. 2 and the multisection taper of Fig. 4a were optimized at a single wavelength of λ_0 =1.55 μm. We found that in both cases the transmission efficiency is close to its maximum value in a broad range of wavelengths. This is due to the fact that in both cases the high transmission efficiency is not associated with any strong resonances. Similar broadband responses are observed in couplers between dielectric waveguides with highly different widths based on multisection tapers,[21,22] and in multisection impedance matching transformers used in microwave circuits.[25]

3.4. Multisection taper for enhanced second harmonic generation

Here we investigate nonlinear devices in which multisection tapers are used as couplers between the MDM and dielectric waveguides. Such couplers can be designed to have almost complete transmission over a broad wavelength range and are optimized to have maximum transmission at the first and second harmonic.

4. CONCLUSIONS

We showed that field enhancement in MDM waveguides can result in large enhancement of SHG. We first considered a structure consisting of a MDM waveguide filled with lithium niobate, which is sandwiched between two high-index-contrast dielectric waveguides. Such a structure forms a Fabry-Perot resonant cavity and can be designed to have a resonance at both the first and second harmonic. We showed that this doubly resonant device results in more than two orders of magnitude enhancement in SHG compared to a uniform slab of lithium niobate. We also considered structures in which multisection tapers are used to couple light in and out of the MDM waveguide. We optimize the tapers so that their transmission efficiency is maximized at both the first and second harmonic. For such structures the field enhancement is due to the squeezing of the optical power from the wavelength-sized dielectric waveguide to the deep subwavelength MDM waveguide.

REFERENCES

1. J. Takahara, S. Yamagishi, H. Taki, A. Morimoto, and T. Kobayashi *Opt. Lett.* **22**, pp. 475–477, 1997.
2. J. C. Weeber, A. Dereux, C. Girard, J. R. Krenn, and J. P. Goudonnet *Phys. Rev. B* **60**, pp. 9061–9068, 1999.
3. J. R. Krenn, B. Lamprecht, H. Ditlbacher, G. Schider, M. Salerno, A. Leitner, and F. R. Aussenegg *Europhys. Lett.* **60**, pp. 663–669, 2002.
4. M. L. Brongersma, J. W. Hartman, and H. A. Atwater *Phys. Rev. B* **62**, pp. R16356–R16359, 2000.
5. S. A. Maier, P. G. Kik, H. A. Atwater, S. Meltzer, E. Harel, B. E. Koel, and A. A. G. Requicha *Nat. Mater.* **2**, pp. 229–232, 2003.
6. S. I. Bozhevolnyi, V. S. Volkov, E. Devaux, and T. W. Ebbesen *Phys. Rev. Lett.* **95**, p. 046802, 2005.
7. E. N. Economou *Phys. Rev.* **182**, pp. 539–554, 1969.
8. J. A. Dionne, H. J. Lezec, and H. A. Atwater *Nano Lett.* **6**, pp. 1928–1932, 2006.
9. S. D. Wu and E. N. Glytsis *J. Opt. Soc. Am. A* **19**, pp. 2018–2029, 2002.
10. G. Veronis, R. W. Dutton, and S. Fan *Opt. Lett.* **29**, pp. 2288–2290, 2004.
11. E. D. Palik, *Handbook of Optical Constants of Solids*, Academic, New York, 1985.
12. J. Jin, *The Finite Element Method in Electromagnetics*, Wiley, New York, 2002.
13. A. Taflove, *Computational Electrodynamics*, Artech House, Boston, 1995.
14. H. Henke, H. Fruchting, and R. Winz *Radio Sci.* **14**, pp. 11–18, 1979.
15. J. A. Porto, F. J. Garcia-Vidal, and J. B. Pendry *Phys. Rev. Lett.* **83**, pp. 2845–2848, 1999.

16. P. Lalanne, J. P. Hugonin, S. Astilean, M. Palamaru, and K. D. Moller *J. Opt. A* **2**, pp. 48–51, 2000.
17. S. Astilean, P. Lalanne, and M. Palamaru *Opt. Commun.* **175**, pp. 265–273, 2000.
18. Y. Takakura *Phys. Rev. Lett.* **86**, pp. 5601–5603, 2001.
19. F. J. Garcia-Vidal, H. J. Lezec, T. W. Ebbesen, and L. Martin-Moreno *Phys. Rev. Lett.* **90**, p. 213901, 2003.
20. M. M. Spuhler, B. J. Offrein, G. L. Bona, R. Germann, I. Massarek, and D. Erni *J. Lightwave Technol.* **16**, pp. 1680–1685, 1998.
21. B. Luyssaert, P. Vandersteegen, D. Taillaert, P. Dumon, W. Bogaerts, P. Bienstman, D. V. Thourhout, V. Wiaux, S. Beckx, and R. Baets *IEEE Photon. Technol. Lett.* **17**, pp. 73–75, 2005.
22. B. Luyssaert, P. Bienstman, P. Vandersteegen, P. Dumon, and R. Baets *J. Lightwave Technol.* **23**, pp. 2462–2468, 2005.
23. K. Krishnakumar *Proceedings of the SPIE* **1196**, pp. 289–296, 1989.
24. B. Wang, J. Jiang, and G. P. Nordin *Opt. Express* **12**, pp. 3313–3326, 2004.
25. D. M. Pozar, *Microwave Engineering*, Wiley, New York, 1998.